Differential glycolytic profile and Warburg effect in papillary thyroid carcinoma cell lines

RAQUEL GUIMARÃES COELHO[1], JULIANA DE MENEZES CAZARIN[1], JOÃO PAULO ALBUQUERQUE CAVALCANTI DE ALBUQUERQUE[1,2], BRUNO MOULIN DE ANDRADE[1,3] and DENISE P. CARVALHO[1]

[1]Laboratory of Endocrine Physiology, Carlos Chagas Filho Institute of Biophysics, Federal University of Rio de Janeiro, Rio de Janeiro 21941-902; [2]Laboratory of Mitochondrial Bioenergetics and Physiology, Medical Biochemistry Institute Leopoldo De Meis, Federal University of Rio de Janeiro, Rio de Janeiro 21044-020; [3]Postgraduate Program of Endocrinology, Medical School, Federal University of Rio de Janeiro, Rio de Janeiro 21941-901, Brazil

Received April 13, 2016; Accepted June 9, 2016

DOI: 10.3892/or.2016.5142

Abstract. Acceleration of glycolysis is a characteristic of neoplasia. Previous studies have shown that a metabolic shift occurs in many tumors and correlates with a negative prognosis. The present study aimed to investigate the glycolytic profile of thyroid carcinoma cell lines. We investigated glycolytic and oxidative parameters of two thyroid carcinoma papillary cell lines (BCPAP and TPC1) and the non-tumor cell line NTHY-ori. All carcinoma cell lines showed higher rates of glycolysis efficiency, when compared to NTHY-ori, as assessed by a higher rate of glucose consumption and lactate production. The BCPAP cell line presented higher rates of growth, as well as elevated intracellular ATP levels, compared to the TPC1 and NTHY-ori cells. We found that glycolysis and activities of pentose phosphate pathway (PPP) regulatory enzymes were significantly different among the carcinoma cell lines, particularly in the mitochondrial hexokinase (HK) activity which was higher in the BCPAP cells than that in the TPC1 cell line which showed a balanced distribution of HK activity between cytoplasmic and mitochondrial subcellular localizations. However, TPC1 had higher levels of glucose-6-phosphate dehydrogenase activity, suggesting that the PPP is elevated in this cell type. Using high resolution respirometry, we observed that the Warburg effect was present in the BCPAP and TPC1 cells, characterized by low oxygen consumption and high reactive oxygen species production. Overall, these results indicate that both thyroid papillary carcinoma cell lines showed a glycolytic profile. Of note, BCPAP cells presented some relevant differences in cell metabolism compared to TPC1 cells, mainly related to higher mitochondrial-associated HK activity.

Correspondence to: Dr Raquel Guimarães Coelho, Laboratory of Endocrine Physiology, Carlos Chagas Filho Institute of Biophysics, Federal University of Rio de Janeiro, Avenida Brigadeiro Trompowski, Rio de Janeiro 21044-020, Brazil
E-mail: raq.gmcoelho@gmail.com; rg.coelho@biof.ufrj.br

Key words: glycolysis, thyroid, Warburg effect, thyroid carcinoma

Introduction

Thyroid carcinoma is the most common malignancy of the endocrine system and is one of the human cancers with the most rapidly increasing prevalence in many countries (1,2). Although the majority of thyroid cancer patients have an excellent outcome, in approximately 10% of patients with well-differentiated thyroid cancer, the ability to respond to radioiodine therapy is lost and poorly differentiated or undifferentiated tumors lead to recurrent disease and death (3,4). The most common thyroid cancer is papillary thyroid carcinoma (PTC) which is classified as a well-differentiated carcinoma and is often curable by the combination of surgery and radioiodine ablation (3-6). However, intense cell progression and aggressive spread of the tumor occur in some patients, leading to loss of the ability to uptake iodine. Thus, in these cases of advanced differentiated thyroid carcinoma, the use of new effective therapeutic strategies is a dilemma (6,7).

Recent studies have shown that molecular alterations at signaling pathways, such as RAS, RAF and mitogen-activated protein kinase (MAPK) are involved in the thyroid neoplastic process (8-11). Furthermore, previous studies have shown that in thyroid cancer, tumor progression is accompanied by increased glucose uptake as detected by ^{18}F-fluorodeoxyglucose positron emission tomography (^{18}F-FDG PET) and decreased radioiodide uptake ability (12). In general, transformed cells have altered energy metabolism (13-17), since in these cells glycolysis is not inhibited in the presence of oxygen. At the beginning of the last century, Warburg reported that cancer cells are able to convert glucose into lactate, even in the presence of oxygen. This phenomenon was called aerobic glycolysis or the 'Warburg effect' (13,14,18). In the following years, it has been shown that in addition to higher glycolytic flux, there is an increased expression of glucose transporters (GLUTs), in parallel with a reduction in oxidative metabolism (13-20). Although the Warburg hypothesis is well

Table I. Primer sequences used for real-time PCR assay.

Gene	Forward	Reverse
GLUT1	CATCAACCGCAACGAGGA	GGTCATGGGTCACGTCAG
HK1	ACATTGTCTCCTGCATCTCTG	GCGTTAAAACCCTTTGTCCAC
HK2	GCAAGGAGATGGAGAAAGGG	AGCACACGGAAGTTGGTC
PFK1p	CATCGACAATGATTTCTGCGG	CCATCACCTCCAGAACGAAG
PFK1l	AACGAGAAGTGCCATGACTAC	GTCCCATAGTTCCGGTCAAAG
PFK1m	TGACCAAAGATGTGACCAAGG	GCGAACCACTCTTAGATACCG
PKM1	ACCGAGCTGTTTGAAGAA	TCCATGAGGTCTGTGGAGTG
PKM2	ATGGCTGACACATTCCTGG	CATCTCCTTCAACGTCTCCAC
LDH	CGTGTTATTGGAAGCGGTTG	TTCATTCCACTCCATACAGGC
PPIA	CCGAGGAAAACCGTGTACTATTAG	TGCTGTCTTTGGGACCTTG

Glut1, glucose transporter 1; HK1, hexokinase isoform 1; HK2, hexokinase isoform 2; PFK1p, phosphofructokinase-1 isoform P; PFK1l, phosphofructokinase-1 isoform L; PFK1m, phosphofructokinase-1 isoform M; PK, pyruvate kinase; LDH, lactate dehydrogenase; PPIA, peptidylprolyl isomerase A.

established, the adaptive mechanisms that lead to decreased oxidative metabolism in cancer cells remain obscure in many carcinoma models.

These features indicate the need to specifically study the metabolic profile of this thyroid tumor type. Few studies have evaluated energy metabolism directly as related to the process of tumorigenesis, although they represent an interesting model of tumor spectra with differing prognoses. Recently, our group demonstrated that thyroid iodide and glucose uptakes are influenced by the energy 'fuel gauge' AMP-activated protein kinase (AMPK) signaling pathway (7). Indeed disruption of cellular energy metabolism is considered a hallmark of cancer in several tumor lineages (18). To our knowledge, however, no study has evaluated tumor cell metabolism behavior in different thyroid cancer cell lineages. In this regard, in the present study we aimed to analyze the metabolic profiles and the activity of key glycolytic enzymes in two thyroid carcinoma cell lines and in one non-tumor human thyroid cell line. Our results strongly suggest that the differences in the glycolytic profile found in these cell lines may explain, at least in part, their different growth rates, which may in turn be associated with more aggressive phenotypes.

Materials and methods

Reagents. 3-(4,5-dimethylthiazol-2-yl)-2,5-diphenyltetrazolium bromide (MTT), glucose, 2-deoxyglucose (2-DOG), nicotinamide adenine dinucleotide phosphate ($NADP^+$), oligomycin (Olig), glucose-6-phosphate dehydrogenase (G6PDH) kit, ATP kit and lactate kit were purchased from Sigma-Aldrich (St. Louis, MO, USA) and Glucox 500 reagent from Doles Reagentes (Goiânia, Goiás, Brazil). All other chemicals were of the highest grade available. Polyvinylidene difluoride (PVDF) membranes were provided by Bio-Rad (Hercules, CA USA) and Millipore (Billerica, MA, USA). Specific antibody against GLUT1 (1:1,000) was from Abcam (Cambridge, MA, USA), and against hexokinase I (HKI) (1:1,000) and HKII (1:1,000) were both purchased from Cell Signaling Technology, Inc. (Danvers, MA, USA). Cell culture medium Dulbecco's modified Eagle's medium (DMEM) and RPMI-1640 were provided by HiMedia Laboratories (Curitida, Brazil) and fetal bovine serum from Invitrogen Life Technologies (Carlsbad, CA, USA).

Cell culture. Human PTC cells (BCPAP and TPC1) and NTHY-ori cell lineages were generous gifts from Dr Corinne Dupuy, (Institut Gustave Roussy, Paris, France). Cells were cultivated in DMEM (BCPAP and TPC1) and RPMI (NTHY), supplemented with 10% bovine serum medium, and maintained at 37˚C in 5% CO_2.

Cell viability. The MTT assay was used to test cell viability in three different experiments. First, we measured the cell viability after 6, 24, 48 and 72 h under a baseline condition. Then, we tested the cytotoxicity after treatment with Olig. In this case, the cells were grown in medium until 80% confluence was achieved. The medium was removed and fresh medium containing 2 μg/ml Olig was added for 2 or 24 h. Also, after the cells achieved confluence, the medium was removed and fresh medium containing 2 mM of 2-DOG was added to the medium for 24 h.

Total mRNA extraction and quantitative RT-PCR. Immediately after treatment, total RNA was extracted using the RNeasy Plus Mini kit (Qiagen Sciences Inc., Germantown, MD, USA) following the manufacturer's instructions. Total RNA was reverse transcribed into cDNA using a high-capacity reverse transcriptase kit (Applied Biosystems Inc., Carlsbad, CA, USA). The specific forward and reverse primers are presented in Table I and were designed to span introns and avoid detection of genomic DNA contamination. Real-time amplifications were carried out using ABI Prism 7500 equipment (Applied Biosystems, Invitrogen Life Technologies, São Paulo, Brazil). The amplification reactions were performed in 96-well plates in 12 μl final volume that contained 3 μl cDNA (diluted 1:100), 7.5 μl of SYBR Master Mix (Applied Biosystems, Invitrogen Life Technologies), and 150 nM of each forward and reverse primers. The amplification program consisted of 55˚C for

2 min, 95˚C for 10 min followed by 40 cycles of 95˚C for 30 sec, and 58˚C for 1 min. The RT-PCR efficiency was evaluated using serial dilutions of the cDNA template, and melting curve data were collected to assess RT-PCR specificity. Each cDNA sample was amplified in duplicate, and a corresponding sample without reverse transcriptase (no-RT sample) was included, as a negative control. The content of the target gene transcripts was normalized to that of peptidylprolyl isomerase A (PPIA). The relative quantities of gene expression were determined by the comparative Ct method expressed by the formula $2^{-\Delta\Delta Ct}$ (19), where Ct refers to the threshold cycle and was determined for each plate by 7500 Real-Time PCR system sequence detection software (Applied Biosystems, Invitrogen Life Technologies).

Glucose consumption and lactate production. Glucose uptake was measured as previously described (20). Cells were cultivated in 6-well plates. After confluence, the cells were washed twice, and glucose (1 mM) was added to the PBS saline solution. Aliquots of the incubation medium were collected each 5 min and transferred to 96-well plates. After 60 min, the glucose concentrations in the samples were analyzed by colorimetric methods (20). The specific glucose uptake was corrected by protein concentration that was evaluated using the BCA protein assay kit (Pierce, Thermo Scientific Fisher, Waltham, MA, USA). Lactate production was recorded using the same cell pool. Cells were lysed and the lactate content was measured by procedures according to the instructions provided by the kit (Sigma Chemical Co.).

ATP content. Cells were cultivated in 12-well plates. After 80% confluence, the medium was removed, and the cells were washed twice, processed using a luciferin-luciferase bioluminescence assay according to the instructions provide by the ADP/ATP ratio assay kit (MAK 135; Sigma Chemical Co.). In the presence of luciferase, ATP immediately reacts with the substrate D-luciferin to produce light. The light intensity is a direct measure of the intracellular ATP concentration.

Western blot analysis. GLUT1, HK1 and HK2 levels were analyzed after lysis of the cells in a buffer [0.05 M Tris-HCl (pH 8.0), 0.15 M NaCl, 0.1% SDS, 0.5% deoxicolic acid, 5 mM $MgCl_2$, Triton 1%, 1 mM PMSF, 1 mM NaF, 1 mM Na_3VO_4, 1 M leupeptin and 1 M pepstatin]. Subsequently, the samples were centrifuged and then the supernatant was collected. An aliquot was used to determine the concentration of protein by the BCA protein assay kit. Fifty micrograms of protein were then resolved on SDS-PAGE gels, transferred to PVDF membranes, and probed with the indicated primary antibodies. We used a β-actin antibody (1:8,000) from Sigma-Aldrich as the loading control. The detection of proteins was performed by chemiluminescence (ECL; Pierce, Thermo Scientific Fisher) following densitometric analysis.

HK activity. Initially, we measured cellular viability by trypan blue and corrected the sample to 10^5 cells. The cells were suspended in lysis buffer [0.05 M Tris-HCl (pH 8.0), 0.15 M NaCl, 0.1% SDS, 0.5% deoxicolic acid, 5 mM $MgCl_2$, Triton 1%, 1 mM PMSF, 1 mM NaF, 1 mM Na_3VO_4] and HK activity was assayed as previously described (7). Blanks with none of the coupled enzymes were performed to control for non-specific oxidation/reduction. For mitochondrial HK fraction assay, the homogenates were centrifuged at 10,000 x g to separate the soluble fraction of HK (total cell extracted) from the particulate fraction (mitochondrial fraction). The HK activity was measured in each cell fraction.

Glucose-6-phosphate content and G6PDH activity. To measure the glucose-6-phosphate (G6P) amount, cells were corrected to 10^5 cells and suspended in lysis buffer [0.05 M Tris-HCl (pH 8.0), 0.15 M NaCl, 0.1% SDS, 0.5% deoxycolic acid, 5 mM $MgCl_2$, Triton 1%, 1 mM PMSF, 1 mM NaF, 1 mM Na_3VO_4]. The reaction medium contained 50 mM Tris-HCl, pH 8.0, 0.5 mM $NADP^+$ and 0.2 U/ml G6PDH. Reduction of $NADP^+$ was followed by measuring the absorbance at 340 nm in a microplate reader (Victor 4 XR; Perkin-Elmer Inc., Waltham, MA, USA). To measure G6PDH activity, cells were corrected to $1x10^5$ cells and suspended in lysis buffer following the instructions of the G6PDH kit assay (Sigma Chemical Co.) measuring the absorbance at 340 nm in a microplate reader (Victor 4 XR; Perkin-Elmer Inc., São Paulo, Brazil).

Pyruvate kinase activity. Samples (10^5 cells) were suspended in lysis buffer [0.05 M Tris-HCl (pH 8.0), 0.15 M NaCl, 0.1% SDS, 0.5% deoxicolic acid, 5 mM $MgCl_2$, Triton 1%, 1 mM PMSF, 1 mM NaF, 1 mM Na_3VO_4] and pyruvate kinase (PK) assay was recorded using the PK kit (Sigma Chemical Co.) measuring the absorbance at 340 nm in a microplate reader (Victor 4 XR; Perkin-Elmer Inc.).

Oxygen consumption. The assay was performed with intact cells (10^6 cells/ml) in culture medium and oxygen consumption rates were measured polarographically using high-resolution respirometry (Oroboros Oxygraph - O_2K; Oroboros Instruments, Innsbruck, Austria). Assay was started by adding cells in the closed (2 ml) respirometer chamber, and the basal respiration status of the different cell lines was collected. Immediately, we added Olig (1 μg/ml), to acquire the oxygen consumption coupled to ATP synthesis calculated by basal O_2 consumption - Olig O_2 consumption. Finally, we add a selective inhibitor form complex IV (KCN 1 mM) to completely block mitochondrial respiration called the residual oxygen consumption.

ROS production. The levels of intracellular ROS were measured using a reactive oxygen species assay kit (Applygen Technologies, Inc., Beijing, China). Briefly, the intracellular formation of ROS in the TPC1 and BCPAP cells was determined using 2'7'-dichlorodihydrofluorescein diacetate (DCFH-DA) molecular probes. DCFH-DA is a membrane-permeable indicator of ROS levels and the reaction between these probes and intracellular ROS yields the fluorescent molecule DCF, which may be used as an indicator of intracellular ROS levels. Cells were washed with PBS and loaded with 10 μM DCFH-DA in serum-free DMEM without phenol red in the dark for 30 min at 37˚C. The excess dye was flushed off and the cells were suspended in serum-free DMEM. Fluorescence intensity was quantified using a BD FACSVantage™ SE (BD Biosciences, Franklin Lakes, NJ, USA).

Statistical analysis. Statistical analyses were performed using GraphPad Software, Inc. (San Diego, CA, USA), and

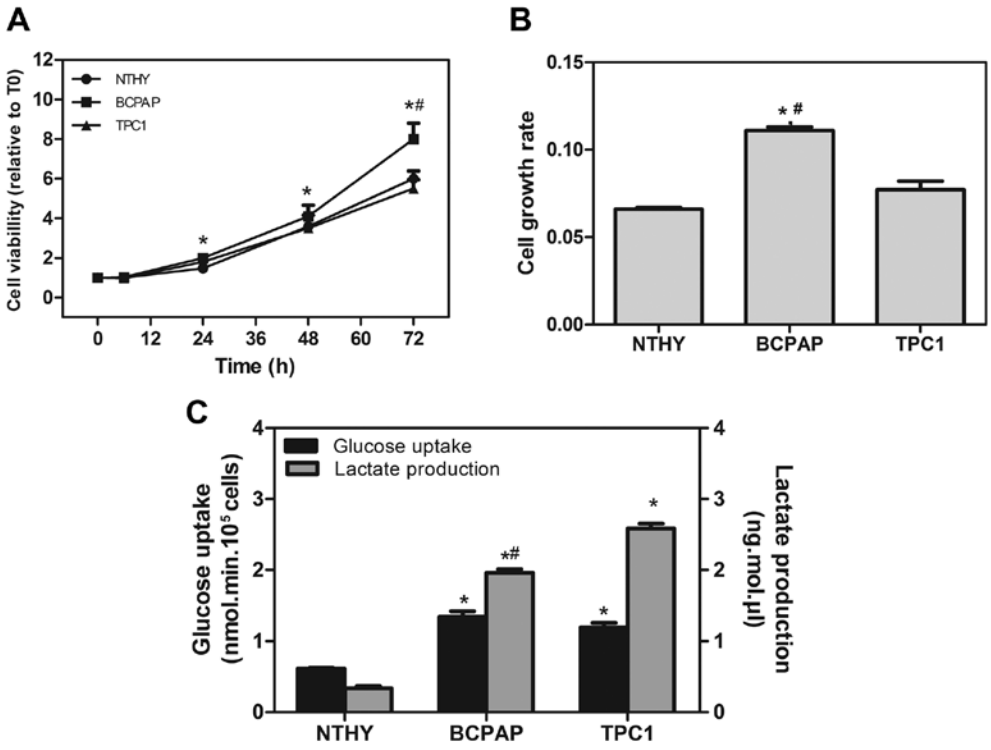

Figure 1. Cell growth and metabolic profile of human thyroid carcinoma cell lines. (A) NTHY-ori, BCPAP and TPC1 cells were seeded (T0) and cell viability was analyzed at 6, 24, 48 or 72 h in baseline condition. (B) The growth rate was measured by MTT considering the time of cell growth from 24 to 48 h. (C) The glucose uptake and intracellular lactate production were measured simultaneously. Data are expressed as mean ± SEM of at least 3 independent experiments $^{*}p<0.05$ compare to NTHY cells; $^{\#}p<0.05$ compared to TPC1 cells (ANOVA followed by Bonferroni post test).

the tests were as follows: Student's t-test or one-way analysis of variance (ANOVA) followed by the Bonferroni multiple comparison test, as described in the figure legends. The level of significance was set at $p<0.05$.

Results

Cell growth pattern and glycolytic capacity among thyroid carcinoma cell lines. In attempt to described differences in energy behavior between thyroid carcinoma cell lineages, we analyzed the cell growth rate and glycolic capacity of all cells (Fig. 1). BCPAP showed a higher cell growth rate different from TPC1 after 48 h (Fig. 1A). Both TPC1 and the non-tumor cell line NTHY-ori exhibited the same growth rate (Fig. 1B). The glucose uptake of tumor cell lines was 2- to 3.5-fold higher than the uptake found in non-tumor cells. The lactate production was also much higher in the BCPAP and TPC1 cell lines when compared to the NTHY-ori cells (Fig. 1C). These data suggest that thyroid carcinoma cell lines show a high ability to convert glucose into lactate (glycolytic efficiency), an important phenomenon possibly involved in tumor survival.

Expression of different glycolytic enzymes and protein expression pattern. To investigate the mechanisms involved in the differences found in the metabolism of these cell lines, we analyzed the mRNA expression and levels of proteins involved in the glycolytic flux. As shown in Fig. 2A, we observed that Glut1 mRNA and protein levels were more highly expressed in both carcinoma cell lines than these levels in the NTHY-ori cells. Moreover, the protein levels of HK1 and HK2 isoforms were more highly expressed in the cancer cell lines (Fig. 2B and C) in the same way as gene expression of other glycolytic targets such as PKM1 and PKM2.

Glycolytic enzyme activity patterns in the thyroid carcinoma cell lines. According to previous results, we analyzed the activity of specific regulatory enzymes of glycolysis and the pentose phosphate pathway (PPP). As shown in Fig. 3A, we observed a higher HK activity pattern in the BCPAP and TPC1 cell lines compared to this pattern in the NTHY-ori cells. However, the amount of G6P in the BCPAP cell line was lower than that in the TPC1 cells, indicating a difference in the use of this substrate (Fig. 3B). As G6P is consumed by both glycolysis and PPP, we evaluated the G6PDH activity, the limiting step enzyme of PPP. Although, the mRNA levels of G6PDH did not differ among all thyroid cell lines (data not shown), we observed a higher G6PDH activity in the TPC1 cells but not in the BCPAP cells (Fig. 3C). Adding to these, we evaluated the PK activity and our results showed that BCPAP and TPC1 differ from each other in PK activity (Fig. 3D).

The activity and cell localization of HK. In Fig. 3A, the HK activity was the same in both thyroid carcinoma cell lines. Nevertheless, their activity was different when we analyzed the specific cell fraction (cytosolic and mitochondrial fractions). In an attempt to evaluate the degree of HK bound to mitochondria, we observed that BCPAP cells had >90% of total HK activity present in the mitochondrial fraction, while NTHY-ori and TPC1 cells had equally distributed HK activity in both cytosolic and mitochondrial fractions (Fig. 3E).

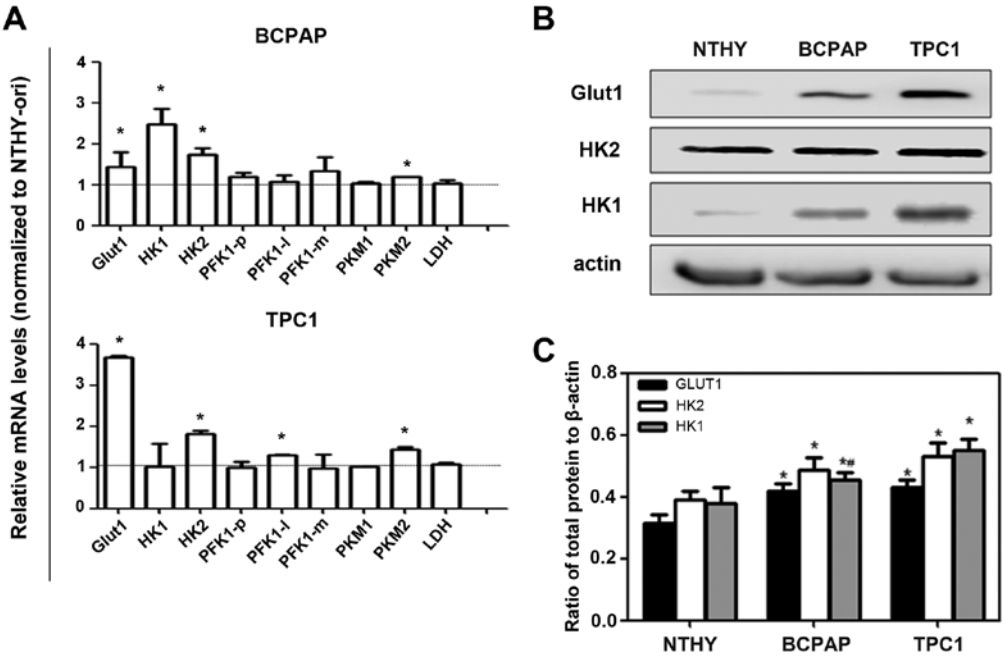

Figure 2. Expression of enzymes involved in energy metabolism of thyroid carcinoma cell lines. (A) Total RNA was extracted from cells and RT-PCR was performed to quantify expression of the indicated genes, using peptidylprolyl isomerase A (PPIA) as endogenous control. Data are expressed as the mean ± SEM of six independent experiments assessing the mRNA expression of: glucose transporter 1 (Glut1), glycolytic enzymes (HK1, hexokinase 1; HK2, hexokinase 2; PFK1-p, phosphofructokinase-1 isoform platelet; PFK1-l, phosphofructokinase-1 isoform liver; PFK1-m, phosphofructokinase-1 isoform muscle; PKM1, pyruvate kinase isoform M1; PKM2, pyruvate kinase isoform M2) and lactate dehydrogenase (LDH) in human thyroid carcinoma cell lines. Results are shown compared to NTHY-ori, a non tumoral cell line; $^{*}p<0.05$. (B) Cell lysates were collected and analyzed by immunoblotting for Glut1, HK1 and HK2 as shown in a representative blot. (C) Data represent means ± SEM of 4 independent experiments using β-actin as a loading control. $^{*}p<0.05$ compared to NTHY-ori and $^{\#}p<0.05$ compared to TPC1 cells.

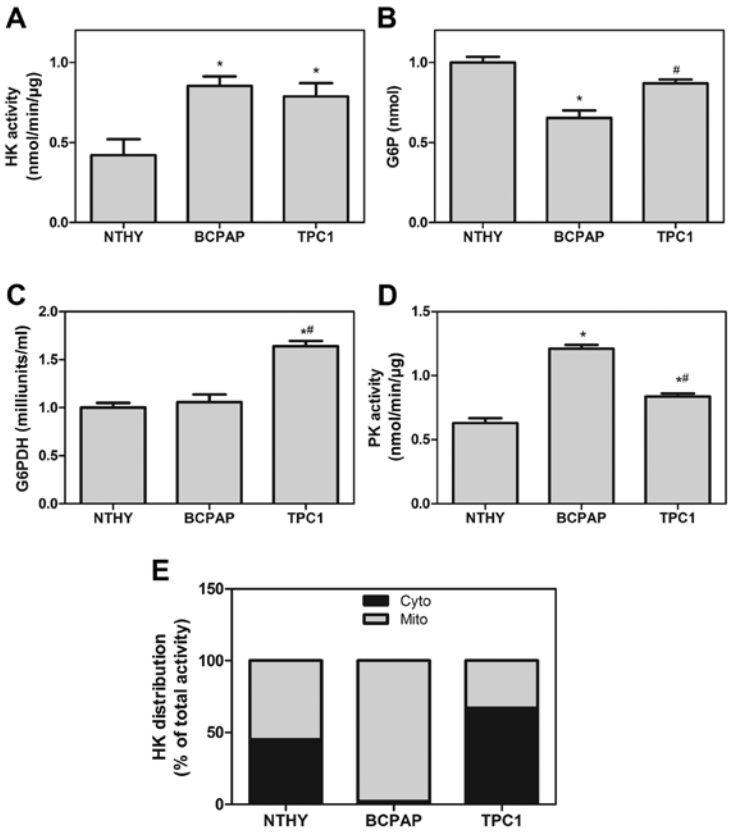

Figure 3. Regulatory glycolytic enzymes and glucose-6-phosphate dehydrogenase (G6PDH) activities in NTHY, BCPAP and TPC1 cells. (A) Total hexokinase (HK) activity, (B) intracellular glucose-6-phosphate (G6P) content, (C) G6PDH activity and (D) specific total pyruvate kinase (PK) activity are expressed as mean ± SEM of 4 independent experiments. $^{*}p<0.05$, a statistically significant difference compared to NTHY cells; $^{\#}$difference between the BCPAP vs. TPC1 cell line, $p<0.05$. (E) The localization of HK activity was measured after differential centrifugation, as described in Material and methods. HK activity in the cytosolic fraction (black bars) and in the mitochondrial fraction (gray bars).

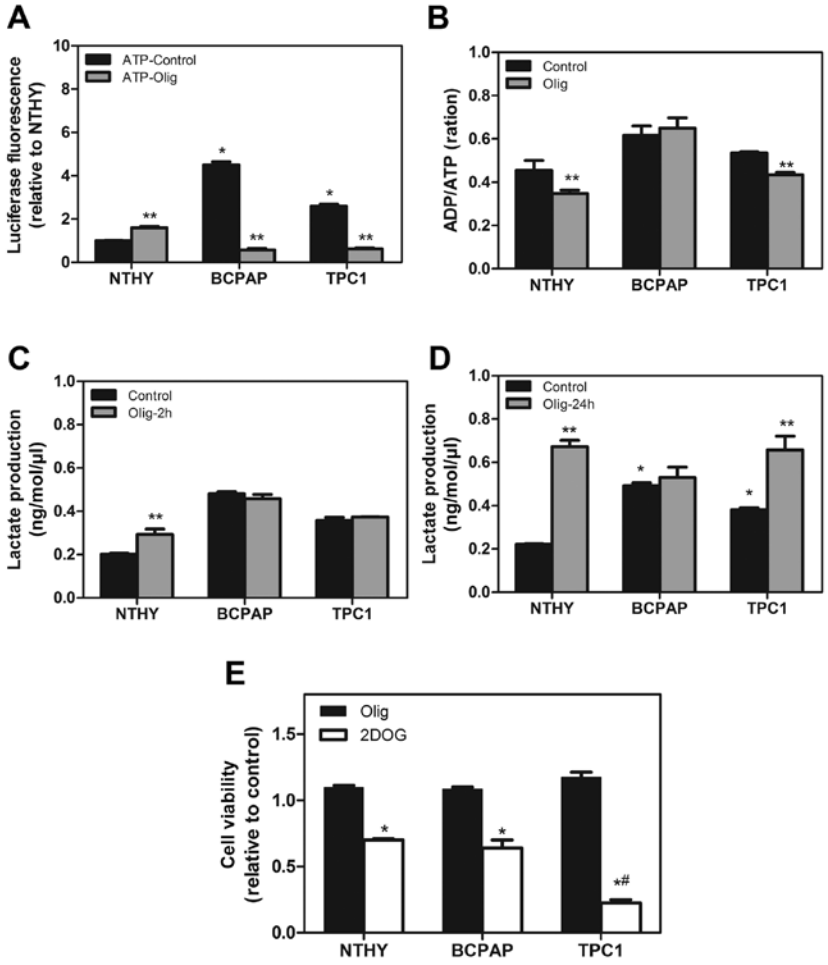

Figure 4. Characterization of anaerobic glycolysis in human thyroid carcinoma cell lines. (A) Intracellular ATP and (B) the ADP/ATP ratio in the presence and absence of 2 μg/ml oligomycin (Olig) for 2 h. The absolute lactate production in the absence or in the presence of 2 μg/ml at 2 h (C) and 24 h (D). Data are expressed as mean ± SEM of 3 independent experiments. *p<0.05 compared to the control (same group) **comparison of ATP levels between cell groups, p<0.05 (black bars) (ANOVA followed by Bonferroni post test). (E) The viability of cells after incubation for 24 h with 2 μg/ml Olig (black bars), and 2 mM of 2-deoxyglucose (2-DOG) (white bars) for 24 h. Data are expressed as mean ± SEM of 3 independent experiments. *p<0.05 compared to the control (without treatment); $^{\#}$p<0.05, difference between the BCPAP vs. TPC1 cell line (white bars) (ANOVA followed by Bonferroni post test).

Characterization of different metabolic pathways for ATP generation. Since our results indicated a high glycolytic potential in these tumor cell lineages, we then evaluated the contribution of the different metabolic pathways for ATP generation in these cells. First, we showed that high levels of ATP and ADP were found in the BCPAP and TPC1 cells in comparison to the NTHY cells (Fig. 4A). Second, we incubated all cells with Olig C, an inhibitor of ATP-synthase complex V of mitochondria electron transport chain, for 2 h. The ATP and ADP levels were reduced following treatment with Olig (Fig. 4A). Moreover, only the NTHY and TPC1 cells showed a modulation of the ADP/ATP ratio in the presence of Olig, suggesting a dependency of mitochondrial oxidative metabolism for ATP generation in TPC1 and non-tumoral NTHY-ori cells (Fig. 4B). On the other hand, Olig treatment caused no modulation in the ADP/ATP content and lactate production in the BCPAP cell line. Yet, the TPC1 cell line showed an increase in lactate production after 24 h in the presence of Olig (Fig. 4C and D). To assess the importance of mitochondrial ATP production to cell viability, we treated the cells with Olig for 24 h or 2-DOG, an inhibitor of glycolytic flux. No differences in cell viability were observed after 24 h of Olig treatment (Fig. 4E) although we found an increase in lactate production in the TPC1 cells at 24 h (Fig. 4D). However, when we inhibited the glycolysis pathway using 2 mM of 2-DOG, we observed a decreased in cell viability after 24 h of incubation in all cell lineages but the effect was more severe in the BCPAP cells when compared with this effect in the TPC1 cells (Fig. 4E).

The Warburg effect is present in PTC cell lines. The above results indicated that the PTC cells are very different. Because of this finding, we evaluated the oxidative profile in all thyroid cell lines. Baseline oxygen consumption in the BCPAP cells was lower than that in the TPC1 cells (Fig. 5A). However, both cell lines showed lower oxygen consumption coupled to ATP production acquired after treatment with Olig (2 μg/ml) (Fig. 5B). These results suggest that these cells could redirect the oxygen to another metabolic pathway. Analysis of residual oxygen, after inhibition of oxidative phosphorylation in tumor cells by KCN (2 mM) showed high residual oxygen consumption by both PTC cells (Fig. 5C). Using a fluorescence probe, we observed that BCPAP and TPC1 cells produced high ROS levels. Moreover, the ROS production by

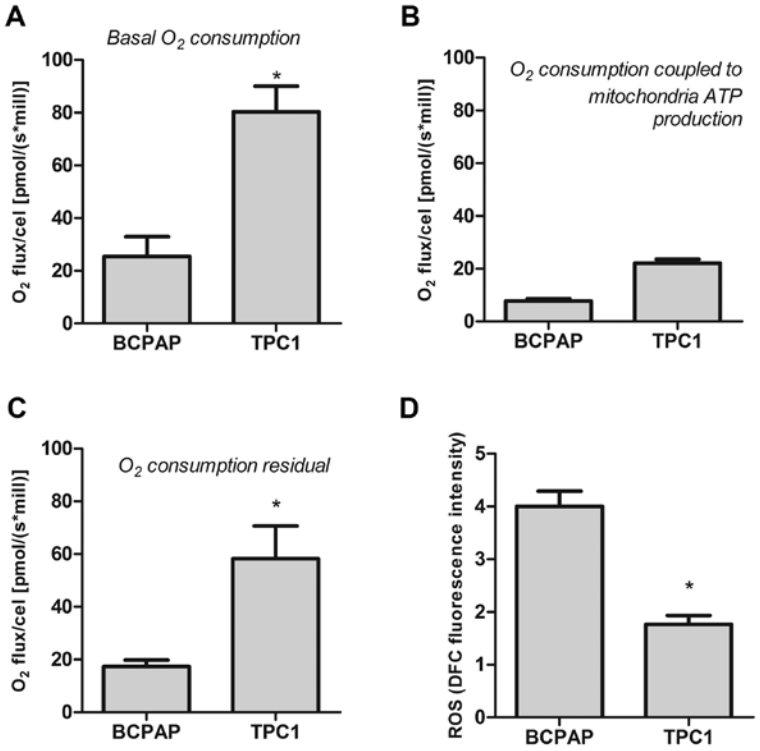

Figure 5. Oxidative metabolism and ROS generation of the BCPAP and TPC1 cell lines. (A) Basal oxygen consumption, (B) oxygen consumption coupled to ATP syntheses and (C) residual oxygen consumption acquired in both cells were monitored as described in Materials and methods. (D) The ROS production was analyzed by DFC fluorescence. Data are expressed as mean ± SEM of at least 5 independent experiments; $^{*}p<0.05$, a significant difference; test-t.

the BCPAP cell line was higher than that noted in the TPC1 cells (Fig. 5D).

Discussion

Although DTC (differentiated thyroid carcinomas) are slow growing tumors with good prognostics, cellular dedifferentiation is present in 20-30% of cases, and is usually accompanied by more aggressive growth, metastatic spread and loss of iodide uptake ability. Cancer growth is a complex process depending on several biological factors, such as the chemical microenvironment of the tumor, its proliferation rate and the cellular metabolic profile. Over the past years, the bioenergetic capacities of tumor cells have been the target of intensive research since many tumors have higher glycolytic rates compared to normal cells (13,18,20-23). As a result, there is a great interest in a better understanding of the cellular mechanisms by which tumor progression and cellular dedifferentiation occur.

Here, we compared the glycolytic parameters in two different cell lines derived from thyroid carcinomas of follicular origin. The TPC1 and BCPAP cells are derived from PTCs, which are responsible for 80-90% of all thyroid malignancies. Although BCPAP and TPC1 cells are derived from the same type of thyroid carcinoma, they show distinct genetic alterations. TPC1 cells show the RET/PTC translocations found in 13-43% of PTCs, which produces constitutive activation of the MAPK pathway (8,9). BCPAP cells present a BRAF V600E mutation, which is a constitutively active serine-threonine kinase that activates MEK1 and MEK2 in the MAPK pathway. This mutation is present in 20-70% of papillary carcinomas (8).

Several studies comparing the glycolytic parameters between tumor and non-tumor cells have demonstrated that the Warburg effect is positively correlated with aggressive behavior, especially in highly proliferative cells (16,17,20-25). Using these thyroid cancer cell lineages, we confirmed this hypothesis, since TPC1 and BCPAP cells presented higher glycolytic efficiency acquired by glucose consumption and lactate production (Fig. 1). Furthermore, the BCPAP cell line has rapid growth rates, representing the typical tumor characteristic. Notably, the TPC1 cell line has the same type of cell adaptations in the glycolytic parameters analyzed, but a lower growth rate when compared to the other thyroid tumor cell types. These results suggest that the differences in glucose metabolism found in tumor cells are not necessarily a consequence of their higher growth rate.

High levels of GLUT1 expression in all cell lineages were observed, which contributed to the elevated glucose uptake and utilization by these cells (Fig. 2). In non-tumor cells, the glycolysis pathway appears to be insufficient to maintain the adequate ATP production rate, since it produces only 2 mol of ATP per mole of glucose (13-15). These cells are usually dependent on metabolic processes that require the oxygen molecule to produce ATP and maintain cell energy demand. Curiously, cancer cells develop a partial anaerobic ability, and thus do not require oxygen for survival despite their fast growth rate (15). According to Gonzalez *et al* (15), this cancer characteristic shifts differentiation to dedifferentiation and proliferative state and some evidence indicates that aerobic glycolysis is closely associated with tumorigenesis and plays an important role in cancer development or malignant characteristics (4,5,15). Our study used models of

two well-differentiated cancer cell lines. Both cell lines had a higher aerobic glycolysis rate, in accordance with previous findings (13-16). Moreover, TPC1 and BCPAP cells had distinct oxidative metabolisms. Both TPC1 and BCPAP showed lower oxygen consumption ATP-coupled (Fig. 5B), indicating that the oxygen consumption of these cells did not drive ATP synthesis. This result could explain the strong inhibitory effect of Olig on ATP levels (Fig. 4A). Yet it is necessary to reinforce that the cell viability 24 h after Olig was not altered in any cells tested. However, the BCPAP cell line was strongly affected by glycolysis inhibition (Fig. 4E), featuring a predominantly glycolytic behavior. Altogether, these results confirm that the phenomenon described by Warburg is also present in thyroid carcinoma cell lineages, no matter the degree of cell differentiation.

However, the TPC1 cell line had a slow growth rate and was dependent on mitochondria for adequate ATP production and survival, despite the higher glycolytic efficiency. On the other hand, BCPAP cells had a high glycolytic efficiency, fast growth rate and were independent of mitochondria for ATP production and survival (Figs. 1 and 4).

Our results also demonstrated that mitochondria were functional in all of the cell types studied. When we used ATP-synthase complex V inhibitor for 2 h, there was a considerable reduction in intracellular ATP levels in all thyroid carcinoma cells. However, the cells were able to reverse the impact exerted by Olig on ATP production after 24 h (data not shown). On the other hand, an opposite effect was observed when we used 2-DOG, an inhibitor of glycolysis (Fig. 4). These results demonstrated that although mitochondrial activity exerted a great influence on cell metabolism, BCPAP cell metabolism was predominantly anaerobic and dependent on the glycolytic phenotype to survive. The TPC1 cells had a predominant mitochondrial dependency to maintain ATP production and their energy status necessary for cell viability. Notably, the TPC1 cell line showed both a glycolytic phenotype and a similar oxidative metabolism. This behavior suggests that TPC1 cells have an intermediate metabolic status, which may explain the less aggressive behavior of these cells. TPC1 cells may have metabolic similarity with normal cells which may contribute to increased resistance to death under stress situations. Chen *et al* (25) demonstrated that breast cancer cells improve their mitochondrial respiratory rate to increase energy production during metastatic processes *in vivo*. Vander Heiden *et al* (18) also described this metabolic phenotype shared with nonmalignant proliferative cells. Furthermore, there is evidence that some solid tumors are able to retain their oxidative capacities, reverting the aerobic glycolysis (12,24-27).

In thyroid tumors, evidence indicates that mitochondrial activities are connected with carcinogenesis, especially in regards to mitochondrial dysfunction (24,26,27). Other mitochondrial functions are also implicated in cell differentiation, in calcium homeostasis, in the production of ROS and regulation of cell death pathways (28,29). In this context, BCPAP and TPC1 cells showed a relationship between glycolytic profiles and ROS production. There are several glycolytic enzymes related to cell survival by mechanisms that involve mitochondrial activity (8,18,24,25). Here, we showed HK activity in all cell lineages. HK is considered as a marker of progression and tumor aggressiveness (23,30,31), and its activation is implicated in maintaining levels of intracellular ATP and suppression of apoptosis (32,34). Although there are four HK isoforms, only HK2 seems to be overexpressed in cancer cells (34). Our results demonstrated that expression of both HK2 and HK1 isoforms was upregulated in the thyroid carcinoma cell lines likewise the specific enzymatic activity in these cells (Figs. 2 and 3), as has been demonstrated in human breast and colorectal cancers (32,33).

HK2 has high affinity for glucose and harbors two catalytic domains that both retain their catalytic activity. In addition, this isoform has an N-terminal domain that allows it to bind to the voltage-dependent anion channel (VDAC), located in the mitochondrial outer membrane. HK2 translocation from the cytoplasm and its binding to the outer mitochondrial membrane produces a complex protein that inhibits apoptosis by preventing the recruitment of pro-apoptotic proteins, such as Bax (34). In addition, HK association to mitochondria exerts a positive regulation on mitochondrial transition pore permeability, limiting the production of ROS and cell death (34).

We thus investigated HK activity in the cytosolic and mitochondrial fraction in thyroid carcinoma cells. The TPC1 cell line has an equal distribution of HK activity in these subcellular fractions different than what we found in the BCPAP carcinoma cells (Fig. 3E). These data suggest that HK associated to mitochondria is upregulated in thyroid carcinoma cells and this mechanism may be involved in glycolysis activation and a fast growth rate.

Hanahan and Weinberg (21) proposed that cancer cells show a reprogramming of metabolic pathways and another glycolytic enzyme that has been studied is PK. Mazurek (35) reported that cancer cells gradually lose the PKM1 isoform and replace it by PKM2. For this reason, PKM2 as well as HK, is considered a link between oncogenes and reprogramming metabolism (30,35). Our results showed that thyroid carcinomas cells had enhanced expression of PKM2 mRNA but not PKM1 mRNA (Fig. 2). Yet, the PK activity in BCPAP cells was higher compared to that noted in the TPC1 cells (Fig. 3). The role of PKM2 in cancer metabolism is to drive the precursors originated during glycolysis to the synthesis of macromolecules and to produce redox potential such as NADPH molecules by PPP.

As far as we are concerned, the mechanisms related to these metabolic changes and the strategies to ensure cell growth and survival, have not yet been unraveled. The literature suggests that the AMPK pathway may play a role in the metabolic changes observed in cancer cells (6,27,29,36,37). AMPK activation has been presented in response to microenvironment energy stress and increased energy consumption in proliferating tumor cells (36). Recently, we demonstrated that AMPK is overexpressed in human PTCs and the cancer cell lines BCPAP and TPC1 have constitutively higher p-AMPK expression than the non-tumor-derived thyroid cell line NTHY-Ori (38). Thus, corroborating Faubert *et al* (37), our results suggest a possible involvement of AMPK in the cellular phenotype found in our research (38).

In conclusion, the metabolic shift described by Warburg in several cancer models was present in the BCPAP and TPC1 cell lines analyzed in our study. However, there were important differences between the PTC cell lines. Better understanding

of the mechanisms involved in this glycolytic phenotype, demonstrated here for the first time, as well as the changes observed in mitochondrial metabolism, could elucidate new therapeutic perspectives for these distinct cell types.

Acknowledgements

This study was supported by grants from the Conselho Nacional de Desenvolvimento Científco e Tecnológico (CNPq), Fundação de Amparo à Pesquisa do Estado do Rio de Janeiro (FAPERJ), and Coordenação de Aperfeiçoamento de Pessoal de Nível Superior (CAPES).

References

1. Davies L and Welch HG: Increasing incidence of thyroid cancer in the United States, 1973-2002. JAMA 295: 2164-2167, 2006.
2. Pilli T, Prasad KV, Jayarama S, Pacini F and Prabhakar BS: Potential utility and limitations of thyroid cancer cell lines as models for studying thyroid cancer. Thyroid 19: 1333-1342, 2009.
3. Pacini F, Cetani F, Miccoli P, Mancusi F, Ceccarelli C, Lippi F, Martino E and Pinchera A: Outcome of 309 patients with metastatic differentiated thyroid carcinoma treated with radioiodine. World J Surg 18: 600-604, 1994.
4. Nikiforova MN and Nikiforov YE: Molecular genetics of thyroid cancer: Implications for diagnosis, treatment and prognosis. Expert Rev Mol Diagn 8: 83-95, 2008.
5. van Staveren WC, Solís DW, Delys L, Duprez L, Andry G, Franc B, Thomas G, Libert F, Dumont JE, Detours V, *et al*: Human thyroid tumor cell lines derived from different tumor types present a common dedifferentiated phenotype. Cancer Res 67: 8113-8120, 2007.
6. Andrade BM and Carvalho DP: Perspective of the AMP-activated kinase (AMPK) signaling pathway in thyroid cancer. Biosci Rep 34: 181-187, 2014.
7. Andrade BM, Cazarin J, Zancan P and Carvalho DP: AMP-activated protein kinase upregulates glucose uptake in thyroid PCCL3 cells independent of thyrotropin. Thyroid 22: 1063-1068, 2012.
8. Kimura ET, Nikiforova MN, Zhu Z, Knauf JA, Nikiforov YE and Fagin JA: High prevalence of BRAF mutations in thyroid cancer: Genetic evidence for constitutive activation of the RET/PTC-RAS-BRAF signaling pathway in papillary thyroid carcinoma. Cancer Res 63: 1454-1457, 2003.
9. Xing M: BRAF mutation in thyroid cancer. Endocr Relat Cancer 12: 245-262, 2005.
10. Nikiforov YE and Nikiforova MN: Molecular genetics and diagnosis of thyroid cancer. Nat Rev Endocrinol 7: 569-580, 2011.
11. Xing M: Molecular pathogenesis and mechanisms of thyroid cancer. Nat Rev Cancer 13: 184-199, 2013.
12. Bläser D, Maschauer S, Kuwert T and Prante O: In vitro studies on the signal transduction of thyroidal uptake of ^{18}F-FDG and ^{131}I-Iodide. J Nucl Med 47: 1382-1388, 2006.
13. Gatenby RA and Gillies RJ: Why do cancers have high aerobic glycolysis? Nat Rev Cancer 4: 891-899, 2004.
14. Warburg O: On respiratory impairment in cancer cells. Science 124: 269-270, 1956.
15. Gonzalez MJ, Miranda Massari JR, Duconge J, Riordan NH, Ichim T, Quintero-Del-Rio AI and Ortiz N: The bio-energetic theory of carcinogenesis. Med Hypotheses 79: 433-439, 2012.
16. Zhao Y, Butler EB and Tan M: Targeting cellular metabolism to improve cancer therapeutics. Cell Death Dis 4: e532, 2013.
17. Amoêdo ND, Valencia JP, Rodrigues MF, Galina A and Rumjanek FD: How does the metabolism of tumor cells differ from that of normal cells. Biosci Rep 33: e00080, 2013. doi: 10.1042/BSR20130066.
18. Vander Heiden MG, Cantley LC and Thompson CB: Understanding the Warburg effect: The metabolic requirements of cell proliferation. Science 324: 1029-1033, 2009.
19. Schmittgen TD and Livak KJ: Analyzing real-time PCR data by the comparative C(T) method. Nat Protoc 3: 1101-1108, 2008.
20. Coelho RG, Calaça IC, Celestrini DM, Correia AH, Costa MA and Sola-Penna M: Clotrimazole disrupts glycolysis in human breast cancer without affecting non-tumoral tissues. Mol Genet Metab 103: 394-398, 2011.
21. Hanahan D and Weinberg RA: Hallmarks of cancer: The next generation. Cell 144: 646-674, 2011.
22. Moreno-Sánchez R, Marín-Hernández A, Saavedra E, Pardo JP, Ralph SJ and Rodríguez-Enríquez S: Who controls the ATP supply in cancer cells? Biochemistry lessons to understand cancer energy metabolism. Int J Biochem Cell Biol 50: 10-23, 2014.
23. Soga T: Cancer metabolism: Key players in metabolic reprogramming. Cancer Sci 104: 275-281, 2013.
24. Vaupel P and Mayer A: Availability, not respiratory capacity governs oxygen consumption of solid tumors. Int J Biochem Cell Biol 44: 1477-1481, 2012.
25. Chen EI, Hewel J, Krueger JS, Tiraby C, Weber MR, Kralli A, Becker K, Yates JR III and Felding-Habermann B: Adaptation of energy metabolism in breast cancer brain metastases. Cancer Res 67: 1472-1486, 2007.
26. Chen JQ and Russo J: Dysregulation of glucose transport, glycolysis, TCA cycle and glutaminolysis by oncogenes and tumor suppressors in cancer cells. Biochim Biophys Acta 1826: 370-384, 2012.
27. Antico Arciuch VG, Russo MA, Kang KS and Di Cristofano A: Inhibition of AMPK and Krebs cycle gene expression drives metabolic remodeling of Pten-deficient preneoplastic thyroid cells. Cancer Res 73: 5459-5472, 2013.
28. Dodson M, Darley-Usmar V and Zhang J: Cellular metabolic and autophagic pathways: Traffic control by redox signaling. Free Radic Biol Med 63: 207-221, 2013.
29. Stankov K, Biondi A, D'Aurelio M, Gasparre G, Falasca A, Romeo G and Lenaz G: Mitochondrial activities of a cell line derived from thyroid Hürthle cell tumors. Thyroid 16: 325-331, 2006.
30. Mathupala SP, Ko YH and Pedersen PL: Hexokinase-2 bound to mitochondria: Cancer's stygian link to the 'Warburg effect' and a pivotal target for effective therapy. Semin Cancer Biol 19: 17-24, 2009.
31. Ros S and Schulze A: Glycolysis back in the limelight: Systemic targeting of HK2 blocks tumor growth. Cancer Discov 3: 1105-1107, 2013.
32. Pastorino JG, Shulga N and Hoek JB: Mitochondrial binding of hexokinase II inhibits Bax-induced cytochrome *c* release and apoptosis. J Biol Chem 277: 7610-7618, 2002.
33. Marini C, Salani B, Massollo M, Amaro A, Esposito AI, Orengo AM, Capitanio S, Emionite L, Riondato M, Bottoni G, *et al*: Direct inhibition of hexokinase activity by metformin at least partially impairs glucose metabolism and tumor growth in experimental breast cancer. Cell Cycle 12: 3490-3499, 2013.
34. Wilson JE: Isozymes of mammalian hexokinase: Structure, subcellular localization and metabolic function. J Exp Biol 206: 2049-2057, 2003.
35. Mazurek S: Pyruvate kinase type M2: a key regulator within the tumour metabolome and a tool for metabolic profiling of tumours. Ernst Schering Found Symp Proc 2007: 99-124, 2007.
36. Vidal AP, Andrade BM, Vaisman F, Cazarin J, Pinto LF, Breitenbach MM, Corbo R, Caroli-Bottino A, Soares F, Vaisman M, *et al*: AMP-activated protein kinase signaling is upregulated in papillary thyroid cancer. Eur J Endocrinol 169: 521-528, 2013.
37. Faubert B, Boily G, Izreig S, Griss T, Samborska B, Dong Z, Dupuy F, Chambers C, Fuerth BJ, Viollet B, *et al*: AMPK is a negative regulator of the Warburg effect and suppresses tumor growth in vivo. Cell Metab 17: 113-124, 2013.
38. Cazarin JM, Coelho RG, Hecht F, Andrade BM and Carvalho DP: 5'-AMP-activated protein kinase regulates papillary (TPC-1 and BCPAP) thyroid cancer cell survival, migration, invasion, and epithelial-to-mesenchymal transition. Thyroid 26: 933-942, 2016.